Environmental Earth Sciences (2018) 77:326
https://doi.org/10.1007/s12665-018-7495-2

ORIGINAL ARTICLE

Determination of the bond–slip relationship of fully grouted rockbolts

Shuqi Ma[1] · Xing Zhu[2] · Weiwei Qin[1] · Shugang Hu[3]

Received: 22 July 2017 / Accepted: 13 April 2018 / Published online: 28 April 2018

Abstract

The bond–slip relationship of fully grouted rockbolts with long encapsulation lengths is critical to the bolt axial performances. However, how to properly determine its profile still remains a challenge. It is proposed that the pullout tests of short encapsulated rockbolts could be used to estimate the bond–slip relationships of long rockbolts under the same conditions. This method is based on two assumptions: (1) The bond–slip relationship simply calculated from the load–displacement curve of a short rockbolt could represent its interfacial shear stress characteristics and (2) bolts with different embedment lengths have the same bond–slip relationship when subjected to the same conditions. Pullout tests were carried out on instrumented rockbolts with short embedment lengths to verify the first assumption, and pullout tests on rockbolts with various embedment lengths were numerically modeled to validate the second assumption. It was found that the shear stresses were not uniformly distributed along the bolt–grout interface; the load–displacement curve of a short rockbolt could still be used to derive the bond–slip relationship of a bolt. The bond–slip relationships computed from short grouted rockbolts tend to underestimate the interfacial shear bond stresses of longer bolts.

Keywords Rockbolt · The bond–slip relationship · Pullout tests · Rockbolt elements

Introduction

The performances of fully grouted rockbolts subjected to tensile loads have been widely studied. Many approaches involving laboratory tests, analytical and numerical methods (Benmokrane et al. 1995; Li and Stillborg 1999; Aziz 2004; Ren et al. 2010; Martin et al. 2011a, b; Ma et al. 2013, 2014a, b, 2016; Ghadimi et al. 2015; Chen and Li 2015; Salemi et al. 2017; Li et al. 2017a, b) are used to study the load transfer mechanism of rockbolts. The bond–slip relationship denotes the relationship of the local shear stress versus the shear slip of the bolt–grout interface. The bond–slip relationships are used in the analytical/numerical analysis of rockbolts (Ivanovic and Neilson 2009; Ren et al. 2010; Martin et al. 2011b; Deb and Das 2011a, b; Ma et al. 2013, 2016; Nemcik et al. 2014; Meng et al. 2015; Tan 2016; Liu et al. 2017). In order to analytically or numerically model the axial behaviors of rockbolts, the interfacial bond–slip relationship is required in advance (Martin et al. 2011b). Benmokrane et al. (1995) pointed out that a trilinear bond–slip model could be used to describe the bond–slip relationship. In this study, 'bond' refers to the interfacial shear bond stress and 'slip' refers to the relative slip between the bolt and grout. The interfacial bond stresses are associated with many factors, such as the steel rebar properties, the host material properties, as well as the grout properties. Aziz (2004) found that the bond stress is affected by the bolt surface profile (rib number and rib space). Zheng et al. (2016) carried out pullout tests on steel bars with encapsulation length of 7–7.5 times the bar diameter. They also found that the number and spacing of ribs on the surface of the steel bar can affect the interfacial bond stress between bar and grout. Li et al. (2017a, b) studied the effects of

✉ Xing Zhu
zhuxing330@163.com

✉ Weiwei Qin
weiwei.qin@swjtu.edu.cn

1 Faculty of Geosciences and Environmental Engineering, Southwest Jiaotong University, Chengdu 611756, People's Republic of China

2 State Key Laboratory of Geohazard Prevention and Geoenvironment Protection (Chengdu University of Technology), Chengdu 610059, People's Republic of China

3 College of Chemical and Environmental Engineering, Shandong University of Science and Technology, Qingdao 266590, People's Republic of China

environmental temperature on the bolt's performance, and they found that the interfacial shear bond stress would distribute more uniformly along the encapsulation length due to the increasing temperature.

Ren et al. (2010) and Martin et al. (2011b), respectively, presented analytical models for rockbolts in which the trilinear bond slip model was adopted. Ma et al. (2013) presented an analytical bolt model based on a nonlinear bond–slip relationship. In addition, numerical studies on the axial behaviors of rockbolts are also carried out. Ivanovic and Neilson (2009) proposed a lumped parameter model taking into account the bilinear and trilinear bond–slip models. Nemcik et al. (2014) improved FLAC2D (Fast Lagrangian Analysis of Continua)'s ability of modeling the axial responses of fully grouted rockbolts by considering the nonlinear bond–slip model.

The bond–slip relationship is of great importance to the axial performances of fully grouted rockbolts. A proper bond–slip relationship which can represent the axial behaviors of bolts is required when accurately modeling the rockbolt behavior. However, it is difficult to determine the value of bond–slip relationship. One method is to do pullout out tests on long strain-gauged bolts (Lu et al. 2018). The interfacial shear bond stress can be computed form the measured strain values, and hence, the local bond–slip relationship can be obtained. Ren et al. (2010), Martin et al. (2011b), Ma et al. (2013), and Huang et al. (2014) analytically computed the bond–slip relationship of a long bolt by best fitting analytical methods with load–displacement curves of bolt pullout tests. The load–displacement curve of the long grouted bolt was required for this method. The problem with the above-mentioned two methods lies in that the long bolt might yield and break during the pullout test as the bolt has high bond strength and long embedment length.

An alternative way to compute the bond–slip relationship of long bolts is to use the short grouted bolts installed under the same installation and geological conditions (Benmokrane et al. 1995; Martin et al. 2011a). Martin et al. (2011a) pointed out that the bond–slip model is the constitutive law of the bolt–grout interface or grout–rock interface, which is not dependent on the embedment length. Wu et al. (2010) presented that the interfacial shear bond stress distribution tends to become uniform with the decrease of the bond length. Yang et al. (2014) obtained the local bond–slip relationship by conducting push-out tests on shortest bond length of 30 mm. They assumed that the shear bond stresses distribute uniformly on the bond length by using the 30 mm bond length.

Once the bond–slip relationship of short grouted rockbolts is obtained, the long bolts installed under the identical conditions are assumed to have the same/similar bonding characteristics. This method is based on two unproven assumptions: (1) The shear bond stress is uniformly distributed along the bolt–grout interface. The mean shear stress is calculated by:

$$\tau = \frac{P}{\pi d_{\mathrm{b}}(L - s)}, \tag{1}$$

where P is the applied load on the bolt; s refers to the bolt displacement; L is the bolt encapsulation length; and d_{b} is the bolt diameter. (2) The computed shear stresses are assumed to be able to represent the interfacial shear stress characteristics of the short bolt; the bond–slip relationships of rockbolts installed under the same conditions, such as the same installing procedure, the same rockbolt and grout used, and the same geological condition of the site, are independent of the bolt embedment length. In other words, bolts with long embedment lengths have the same bond–slip relationship as the short bolts.

Short encapsulation length was defined as less than four times the bolt diameter by Benmokrane et al. (1995), as this encapsulation length could result in uniform bond stress distribution along the bolt–resin interface. Martin et al. (2011a) stated that the encapsulation length which could ensure uniform bond stress is categorized as short encapsulation length.

For the first assumption, in despite of its wide use in practices, little effort has been made to verify its correctness. For instance, the shear bond stress is assumed to be uniform along the short bolt in the studies of Wu et al. (2010) and Yang et al. (2014). The current study is going to experimentally and numerically evaluate this assumption. Two instrumented short rockbolts were pulled out, and the strain values were recorded during the tests. The bond–slip relationships calculated from the strain results were compared to the ones derived from the load–displacement curves. It was found that shear stresses were not uniform along the bolt–grout interface. In other words, the bolt had different interfacial shear stresses at different location along bolt axis.

For the second assumption, Martin et al. (2011a) and Kilic et al. (2002) experimentally investigated effects of the embedment length on the bond strength of bolts installed under identical conditions. They found that the bond strength of rockbolts is independent of the embedment length. However, Li et al. (2016)'s tests showed that the bond strength of rockbolts is related to the embedment length. In the current study, Martin et al. (2011a) and Li et al. (2016)'s test results are used to validate the second assumption. Kilic et al. (2002) did not present the details of the load–displacement relationships of the pullout tests; hence, their tests are not included herein. The load–displacement curves of short grouted bolts were converted to the bond–slip relationships, which were implemented into numerical rockbolt models to predict the axial behavior of long grouted rockbolts. The obtained numerical results were compared to the experimental results of long grouted rockbolts.

The following will first briefly introduce the used numerical method and then present the verifications of the first assumption and the second assumption.

Rockbolt elements in FLAC2D

Rockbolt elements provided in FLAC2D cannot model (without modification) the nonlinear behavior of interfacial shear stress of rockbolts. Nemcik et al. (2014) presented a way to modify the shear stress along the rockbolt element as a function of relative shear displacement using

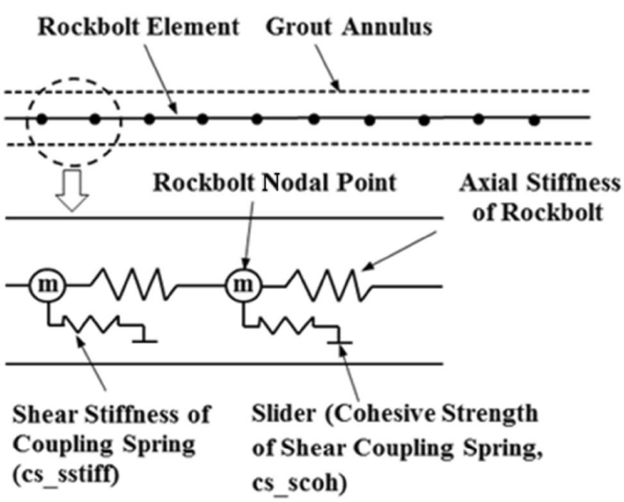

Fig. 1 FLAC rockbolt element with the shear coupling springs

FISH subroutine (a programing language embedded within FLAC). Rockbolt elements transfer the mobilized shear forces to the FLAC grid via shear coupling springs. Figure 1 schematically shows the conceptual mechanical model of rockbolt elements with the shear coupling springs.

The interfacial shear forces generated between the rockbolt elements and the grid are calculated using the coupling spring shear stiffness (cs_sstiff shown in Fig. 2):

$$\frac{F_{\mathrm{S}}}{L} = \mathrm{cs}_{\mathrm{sstiff}}\left(u_{\mathrm{p}} - u_{\mathrm{m}}\right), \tag{2}$$

where F_{S} (N) is the shear force developed in the shear coupling spring; $\mathrm{cs}_{\mathrm{sstiff}}$ (N/m/m) is the coupling spring shear stiffness (in FLAC: cs_sstiff); u_{p} (m) refers to the axial displacement of the rockbolt element; u_{m} (m) is the axial displacement of the medium (soil or rock); and L (m) is the length of the contributing rockbolt element.

The maximum shear force of the rockbolt element is defined by the cohesive strength of the interface and the friction along the interface:

$$\frac{F_{\mathrm{S}}^{\max}}{L} = \mathrm{cs}_{\mathrm{scoh}} + \sigma_C' \tan\left(\mathrm{cs}_{\mathrm{sfric}}\right) \text{ perimeter}, \tag{3}$$

where $\mathrm{cs}_{\mathrm{scoh}}$ (N/m) denotes the cohesive strength of the shear coupling spring (in FLAC: cs_scoh); σ_C' (N/m^2) denotes the mean effective confining stress normal to the rockbolt element; $\mathrm{cs}_{\mathrm{sfric}}$ is the friction angle of the shear coupling spring (in FLAC: cs_sfric); and perimeter (m) is the exposed perimeter of the element.

The shear force per rockbolt length, defined by cs_scoh, can be related to the relative shear displacement by a user-defined table cs_sctable. Hence, the shear bond stress of the rockbolt element can be defined as a function of the relative

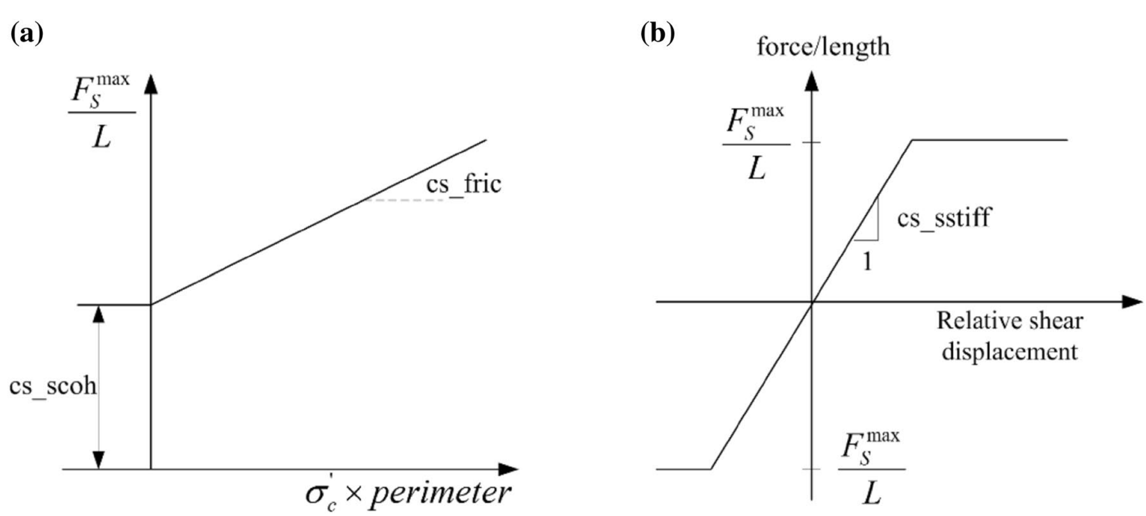

Fig. 2 Behavior of shear coupling springs of rockbolt element, after Itasca (2006). **a** Shear strength criterion, **b** shear force versus displacement

shear displacement using cs_sftable. This provides a way to implement a certain bond–slip relationship into a FLAC model. In this study, cs_sfric was set to zero and the shear force in Eq. (3) is only dependent on cs_scoh.

In FLAC2D, cs_scoh (with the unit of force/rockbolt length) is defined as the cohesive strength of shear coupling spring:

$$\text{cs\_scoh} = \pi d_{\mathrm{b}} \tau \tag{4a}$$

and the corresponding shear stress τ can be computed by:

$$\tau = \frac{\text{cs\_scoh}}{\pi d_{\mathrm{b}}}, \tag{4b}$$

where d_{b} is the rockbolt diameter and τ is the shear stress along the rockbolt.

The bond–slip relationship can be converted to the relationship of shear force per length versus displacement by Eq. (4a).

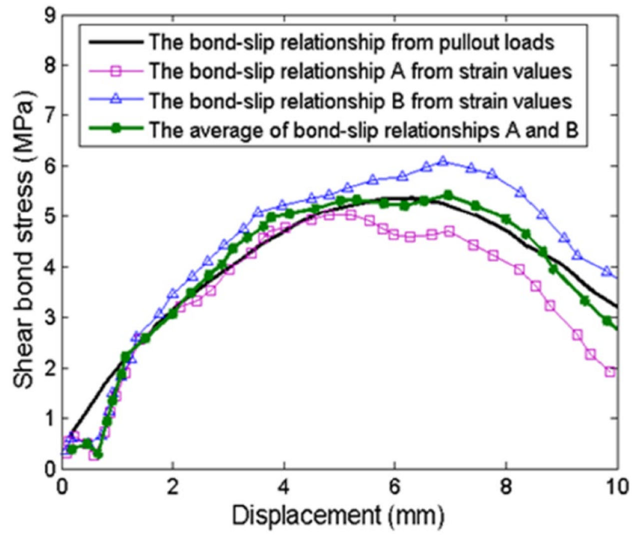

Fig. 3 Comparisons of bond–slip relationships computed from strain values and pullout loads for 130-mm-long bolt encapsulation

Pullout tests on instrumented short bolts

Pullout tests were conducted on short encapsulated bolts with strain gauges measuring the strains developed on the bolt at three different locations. Bolts 20 mm in diameter were grouted in 75- and 130-mm-long steel sleeves using a polyester resin, respectively. Resin of weaker strength was used in the case of 130-mm-long sleeve to avoid the tensile failure of rockbolts. These bolts were pulled out, and the load, displacements, and the strain values were recorded in a computer.

The elastic modulus of bolts is 180 GPa. To prevent strain gauges from being damaged during the test, strain gauges were attached to a small slot which runs along the length of the bolt. The mean shear stress between two strain gauges along the bolt was calculated based on the obtained strain values by the following equation:

$$\tau_i = \frac{E r_{\mathrm{b}} \left(\varepsilon_{i+1} - \varepsilon_{i-1} \right)}{2l}, \tag{5}$$

where l is the gauge separation; E is the elastic modulus of the bolt; and r_{b} is the bolt radius.

130-mm-long bolt encapsulation

Shear stresses were computed from the recorded strain values. The shear stress versus the displacement curves of 130-mm-long bolt are shown in Fig. 3. The average of these two shear stresses is also shown in Fig. 3. The pullout loads applied on the bolt were converted to shear stress by Eq. (1) and are shown in Fig. 3. As can be seen, the two shear bond stress–slip curves (labeled as A and B in Fig. 3) calculated from strain values have different profiles and the average of these two bond–slip relationships A and B agrees well with the one calculated from pullout loads. The shear bond stress–slip curves A and B represent the evolution of the interfacial shear stress at different bolt locations. The discrepancy in the shear stresses generated along the bolt might be caused by the different confinement provided by the steel sleeve. According to the visual observation during the test, the steel sleeve was more deformed at the loaded end of the bolt than at the other end.

Notice that the 'displacement' in Fig. 3 represents the displacement of the loaded end of the bolt and the 'relative slip' in the bond–slip relationships A and B is considered to be equal to the 'displacement,' as the bolt elastic deformation is very small and can be ignored for the 130 mm bolt encapsulation.

A numerical pullout test on a 130-mm-long bolt was carried out using the rockbolt elements in FLAC2D. The two bond–slip relationships A and B were converted to cs_scoh versus displacement relationship, which can be readily implemented into FLAC model. For the reason of simplicity, half of the bolt encapsulation used the bond–slip relationship A and the other half used the bond–slip relationship B. The input numerical parameters are listed in Tables 1 and 2.

The modeled pullout load versus the displacement of the bolt is shown in Fig. 4. Also shown in Fig. 4 is the pullout load versus displacement curve from the laboratory test. The numerical results have a reasonable agreement with the laboratory test.

The bond–slip relationship computed from pullout loads (the load–displacement curve) was also implemented in the numerical modeled pullout test in which the whole bolt was assumed to have an identical bond–slip

Table 1 Simulation model input parameters

Cross-sectional area (m^2)	Elastic modulus (Pa)	Perimeter of the rockbolt (m)	cs_sstiff (N/m/m)	Tensile yield strength (N)	Number of rock-bolt elements for 75 mm bolt	Number of rock-bolt elements for 130 mm bolt
3.14E−04	1.80E+11	0.0628	1.00E+9	200E+3	8	15

Table 2 Input parameters of the concrete in the model

Elastic bulk modulus (Pa)	Elastic shear modulus (Pa)	Mass density (kg/m^3)
5.0E+9	3.0E+9	2000

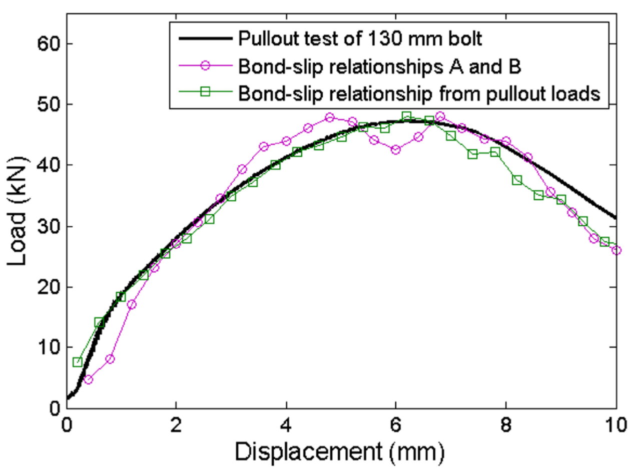

Fig. 4 Comparisons of load–displacement relationships of numerical pullout tests and the laboratory test for 130-mm-long bolt encapsulation

relationship. The resulted load versus displacement curve agrees well with the laboratory results, as well as the numerical results based on the two bond–slip relationships A and B. It indicates that the bond–slip relationship simply computed from the pullout loads could represent the interfacial bond features of rockbolts and is able to predict the axial behaviors of rockbolts.

The coupling spring shear force and shear displacement were recorded during the numerical pullout tests. The shear forces were converted to shear bond stresses by Eq. (4b). The bond–slip relationship curves resulting from the numerical tests are compared to their corresponding input relationships as shown in Fig. 5. It can be seen that the obtained bond–slip relationships agree well with the input relationships, indicating that the FLAC rockbolt elements can closely represent the input bond–slip curves.

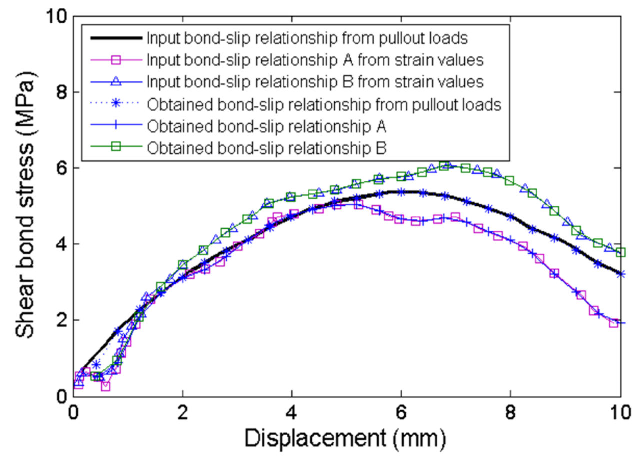

Fig. 5 Comparisons of bond–slip relationships computed from numerical models and the input bond–slip relationships

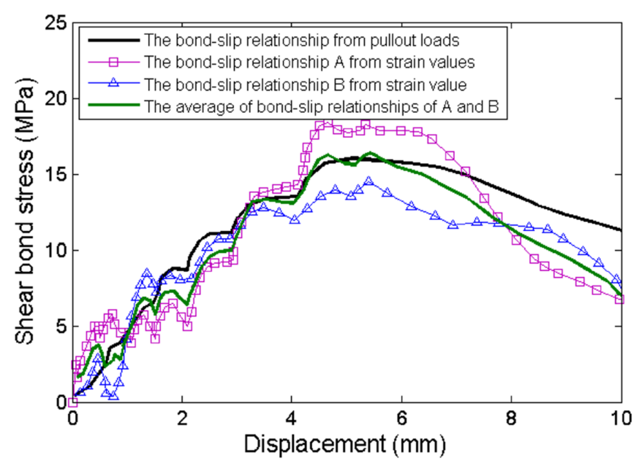

Fig. 6 Comparison of bond–slip relationships computed from strain values and pullout loads for 75-mm-long bolt encapsulation

75-mm-long bolt encapsulation

A 75-mm-long bolt encapsulation was pulled out in a way that the machine would pause and hold the bolt for a few seconds at pullout loads of 20, 30, 40, 50, and 60 kN, respectively. The bond–slip relationships (labeled as A and B) computed from strain values are shown in Fig. 6, in comparison with the bond–slip relationship from pullout loads. The average of the bond–slip relationships A and B is shown

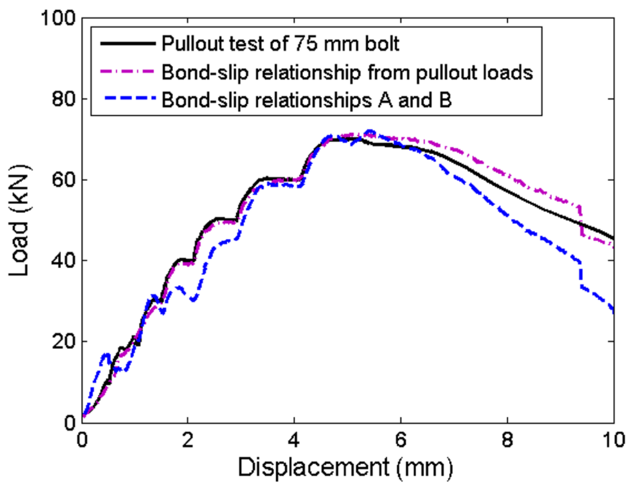

Fig. 7 Comparisons of load–displacement relationships of numerical pullout tests and the laboratory test for 75-mm-long bolt encapsulation

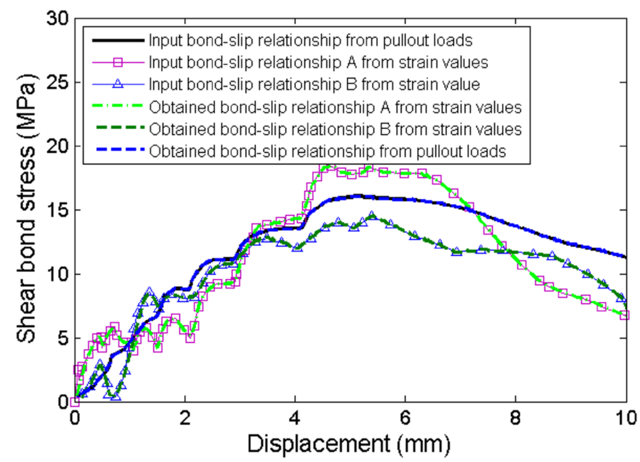

Fig. 8 Comparisons of bond–slip relationships computed from numerical models and the input bond–slip relationships

in Fig. 6, and it can be seen that the averaged bond–slip relationship is close with the one derived from pullout loads.

A numerical pullout test was carried out on the bolt 75 mm in length. The input parameters are the same as in the numerical model of the 130-mm-long bolt as shown in Tables 1 and 2, except for the number of rockbolt elements (eight rockbolt elements for 75-mm-long bolt and 15 rockbolt elements for 130-mm-long bolt). The two bond–slip relationships A and B were implemented in the numerical model. Figure 7 shows the load versus displacement relationships of the numerical pullout tests and the laboratory test. It can be seen that the bond–slip relationships derived from the strain values produce a reasonable agreement with the pullout tests.

Another numerical pullout test with the implementation of the bond–slip relationship calculated from the pullout tests was also conducted. Its load–displacement matches well with the laboratory test as shown in Fig. 7. The bond–slip relationships obtained from numerical models are compared with the input bond–slip relationships as shown in Fig. 8. The obtained numerical bond–slip relationships are in good agreement with their corresponding input bond–slip curves.

Based on the analysis of the results, the findings are: (a) The measured shear stresses are not the same along the embedment length for short encapsulated rockbolts, which might be due to non-uniform confinement provided by the steel tubes, or due to the fact that the bolt embedment lengths are not short enough; (b) the bond–slip relationship derived from the load–displacement curve is in a reasonable agreement with the average of the measured shear stress–shear slip relationships and can generate good predictions on axial behaviors of rockbolts. This leads to that the interfacial shear bonding characteristics of rockbolts could be simply estimated from the load–displacement curves of short encapsulated rockbolts; (c) the rockbolt elements in FLAC2D can successfully represent the input bond–slip relationship and predict well the pullout behaviors of rockbolts.

The testing results are based upon rockbolts installed in steel tubes representing the confinement of concrete/rock mass. The above conclusions need to be further verified by pullout tests on short instrumented rockbolts installed in concrete. Besides, rockbolts with shorter embedment lengths might be considered in the future tests.

Prediction of longer bolts using the bond–slip relationships from short bolt pullout tests

The experiments conducted by Martin et al. (2011a) and Li et al. (2016) are used to demonstrate the potential application of the bond–slip relationship derived from short encapsulated bolts.

Martin et al. (2011a)'s pullout tests

Martin et al. (2011a) conducted two pullout tests on rockbolts with different embedment lengths. They were installed using the resin grout, under an identical confining pressure of 1.2 MPa. The two embedment lengths were 90 and 130 mm, respectively. The diameter of the bolts is 25 mm, and Young's modulus is 160 GPa. The load versus displacement curves of the two bolts are shown in Fig. 9.

The load versus displacement relationship of the 90-mm-long bolt was converted to shear stress versus displacement by Eq. (1), which is shown in Fig. 10. This computed bond–slip relationship was implemented into the FLAC model. Two numerical pullout tests were conducted to

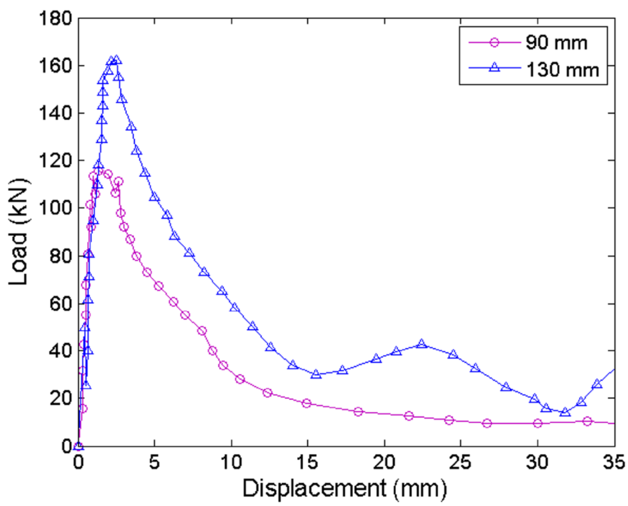

Fig. 9 Load–displacement relationships of two rockbolts, after Martin et al. (2011a)

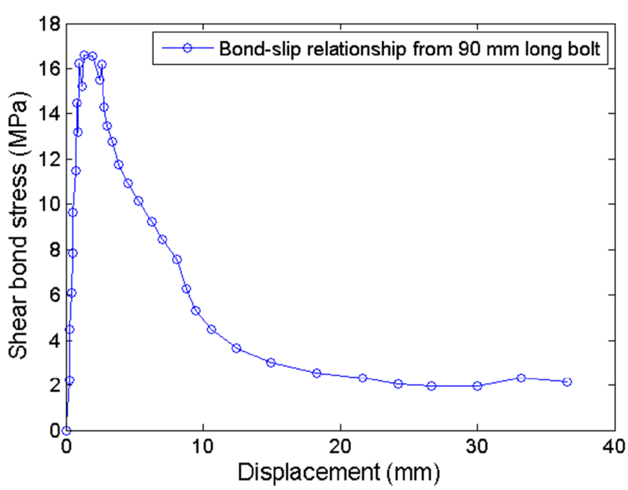

Fig. 10 Bond–slip relationship of 90-mm-long bolt

model the axial behaviors of rockbolts with lengths of 90 and 130 mm, respectively, using the bond–slip relationship derived from the 90 mm rockbolt. The input parameters in FLAC simulation are shown in Table 3. The concrete parameters are listed in Table 2.

The pullout load versus displacement curves obtained from the FLAC rockbolt model are shown in Fig. 11, in comparison with laboratory tests. It can be seen that the numerical model of the 90-mm-long bolt matches well with its corresponding experimental pullout test. Moreover, the numerical model of 130-mm-long bolt shows a good agreement with the pullout test, indicating that the bond–slip model derived from short encapsulated bolts is able to predict the pullout behavior of bolts having longer embedment length. However, as pointed out by Martin et al. (2011a), this conclusion needs to be further verified by more tests.

Li et al. (2016)'s pullout tests

Li et al. (2016) carried out pullout tests on 20-mm-diameter bolts, which are widely used in Norway. The bolts started to yield around 170 kN (Kristjansson 2014). Bolts with varying embedment lengths were grouted with water-to-cement ratios of 0.40, 0.46, and 0.50. These bolts were installed in the concrete with the UCS of approximately 110 MPa. The grout curing time for all the tests ranges from 7 to 9 days, and hence, the grout strength in each test should be the same and have little impact on the bolt pullout behavior. These pullout tests could be considered under the same installation and confinement conditions, and the results are suitable to verify the second assumption. The bond–slip relationships computed from the load–displacement curves of the 10-cm-bolt pullout tests were implemented into numerical rockbolt models with varying embedment lengths. Tables 4 and 5 show the input parameters of the numerical bolt models.

Water–cement ratio 0.40

The pullout load–displacement curves of rockbolts grouted with a water–cement ratio of 0.40 are shown in Fig. 12. The load–displacement curve of bolt B212 (embedment length of 10 cm) in Fig. 12a was converted to the bond–slip relationship, which was implemented into the numerical rockbolt models with embedment lengths of 10, 15, 20, and 30 cm. The predicted load–displacement curves of numerical bolt models with various embedment lengths are shown in Fig. 12.

As can be seen in Fig. 12a, the numerical bolt model of the bolt with the embedment length of 10 cm agrees well with the axial behavior of bolt B212. The numerical bolt model produces a reasonable agreement with bolts having embedment length of 15 cm, as shown in Fig. 12b. For the

Table 3 Simulation model input parameters for Martin et al. (2011a)

Cross-sectional area (m^2)	Elastic modulus (Pa)	Perimeter of the rockbolt (m)	cs_sstiff (N/m/m)	Tensile yield strength (N)	Number of rockbolt elements for 90 mm bolt	Number of rockbolt elements for 130 mm bolt
4.9E−04	1.60E+11	0.078	1.00E+9	200E+3	10	15

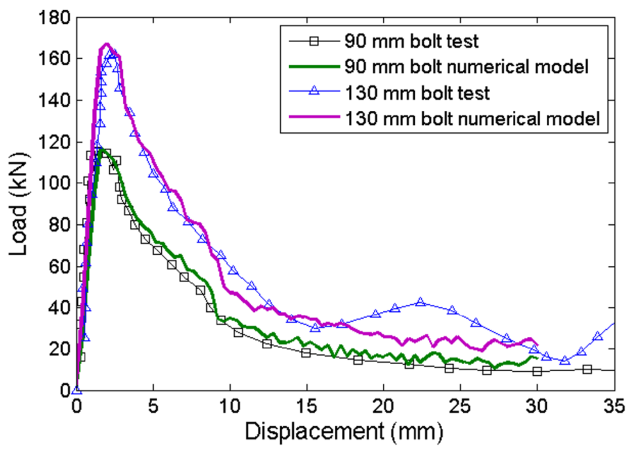

Fig. 11 Comparisons of load–displacement relationships of numerical models and the laboratory test for 90- and 130-mm-long bolts

Table 4 Simulation model input parameters for Li et al. (2016)

Cross-sectional area (m^2)	Elastic modulus (Pa)	Perimeter of the rockbolt (m)	cs_sstiff (N/m/m)	Tensile yield strength (N)
3.14E−04	1.80E+11	0.0628	1.00E+9	170E+3

Table 5 Number of rockbolt elements used in bolt models with different embedment lengths, for Li et al. (2016)

Number of rockbolt elements for 10 cm bolt	Number of rockbolt elements for 15 cm bolt	Number of rockbolt elements for 20 cm bolt	Number of rockbolt elements for 25 cm bolt	Number of rockbolt elements for 30 cm bolt
10	15	20	25	30

embedment length of 20 cm, the bolt in the experimental pullout test yields at 170 kN, whereas the maximum axial load of the numerical test is around 160 kN, less than the yielding strength, as shown in Fig. 12c. It indicates that the numerical bolt model underpredicts the axial loads of the bolt with the embedment length of 20 cm. With the embedment length increasing to 30 cm, the numerical bolt also yields at 170 kN, showing a good match with the experimental results, as shown in Fig. 12d. It should be noted that in Fig. 12d, the bolt material yielding mechanism, rather than the interfacial bonding stress characteristics, predominantly influences the bolt axial behavior. Hence, the good match between the numerical model and experimental tests does not necessarily mean the bond–slip relationship of B212 could predict well the pullout behavior of the bolt with the embedment length of 30 cm.

Water–cement ratio 0.46

The pullout load–displacement curves of rockbolts grouted with a water–cement ratio of 0.46 are shown in Fig. 13. The load–displacement curve of bolt B312 (embedment length of 10 cm) in Fig. 13a was converted to the bond–slip relationship, which was then implemented into the rockbolt models with bolt lengths of 10, 20, 25, and 30 cm. Also shown in Fig. 13 are the resultant numerical load–displacement curves for various embedment lengths. It can be seen from Fig. 13 that the numerical bolt model underpredicts the pullout loads of rockbolts with embedment lengths of 20, 25, and 30 cm.

The load–displacement curve of bolt B322 (embedment length of 20 cm) in Fig. 13b was converted to the bond–slip relationship. The numerical rockbolt models with the B322 bond–slip relationship produce better predictions on bolts with embedment lengths of 25 and 30 cm, which are shown in Fig. 13c, d, respectively.

Water–cement ratio 0.50

The load–displacement curves of rockbolts grouted with a water–cement ratio of 0.50 are shown in Fig. 14. The load–displacement curves of bolts B512 and B513 in Fig. 14a were used in the numerical bolt models. The resultant numerical load–displacement curves are shown in Fig. 14.

It can be seen in Figs. 14b–d that the numerical bolt models with the implementation of bond–slip relationship derived from bolt B512 are in reasonable agreements with the experimental tests of rockbolts with embedment lengths of 20, 30, 40 cm.

The numerical bolt models with the bolt B513's bond–slip relationship underestimate the axial loads of bolts with embedment lengths of 20 and 30 cm. The numerical model of the bolt with embedment length of 40 cm yields at 170 kN and agrees well with the experimental pullout test.

In comparison, the bond–slip relationship derived from the larger load–displacement curve (bolt B512) could lead to better predictions on the axial behavior of bolts with longer embedment length.

It can be seen from Figs. 12c, 13c, and 14c that the numerical bolt models with the bond–slip relationship derived from short embedment length tend to underestimate performance of bolts with longer embedment lengths. This indicates that the bond–slip relationship from short embedment length bolts is smaller than that of bolts with longer embedment length. The bond–slip relationship is affected by its embedment length. Although the bolt installation conditions are similar for bolts with different embedment lengths, their interfacial shear bond stress seems to be dependent of the embedment length. Figure 15 shows the fractures

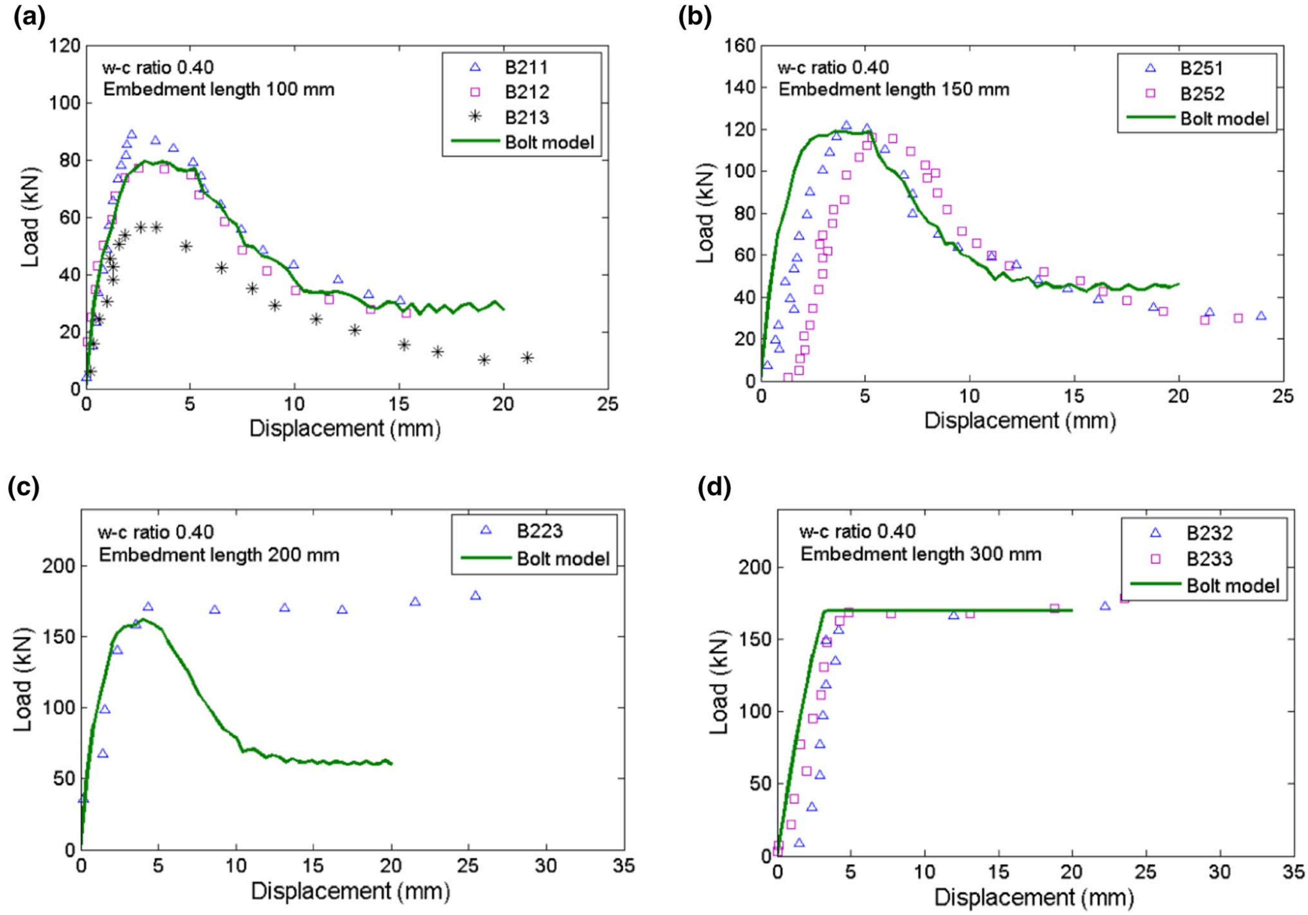

Fig. 12 Load–displacement curves of rockbolts grouted with water–cement ratio of 0.40 in embedment lengths **a** 10 cm, **b** 15 cm, **c** 20 cm, **d** 30 cm

generated during the pullout tests of rockbolts. The resultant pullout loads of rockbolts obliviously include the loads which induced the concrete fractures. The confining concrete contributes to the axial performances of rockbolts. However, the contributions of the concrete to rockbolts with different embedment lengths might be different, which explains why the interfacial bond stress is associated with the embedment length.

The bond–slip relationship obtained from the short bolts tends to underestimate the tensile behaviors of rockbolts having longer embedment lengths. To determine the bond–slip relationship of rockbolts installed in the same/similar conditions, pullout tests of rockbolts with different short embedment lengths should be conducted. For instance, in case of water–cement ratio of 0.46, the bond–slip relationship derived from the bolt with embedment length of 10 cm (B312) underpredicts the axial loads of longer bolts, whereas the bond–slip relationship of the 20-cm-long bolt (B322) generates closer agreement. Hence, the bond–slip relationship computed from the bolt with embedment length of 20 cm should be used in the analysis in order to achieve more accurate results. In case of water–cement ratio of 0.50, the bond–slip relationship computed from bolt B512 generates better predictions on the bolts with longer embedment lengths than the bond–slip relationship of bolt B513. Hence, the bond–slip relationship of bolt B512 should be adopted in the analysis.

To the best of the author's knowledge, there is no proper method for determining the bond–slip relationship of bolts in the literature. The load–displacement curves of short grouted rockbolts are still a good method to estimate the bond–slip relationship of bolts. A series of pullout tests on short grouted bolts need to be carried out in order to evaluate and select a proper bond–slip relationship which could more closely represent the true bond–slip relationship of rockbolts with longer embedment length.

It is generally accepted that the confining stress acting normally to the length of the bolt could influence the bond–slip relationships. This study does not take into account the effects of the confining stress on the bond–slip relationship of bolts. This limitation can be easily overcome via conducting pullout tests under the particular geological

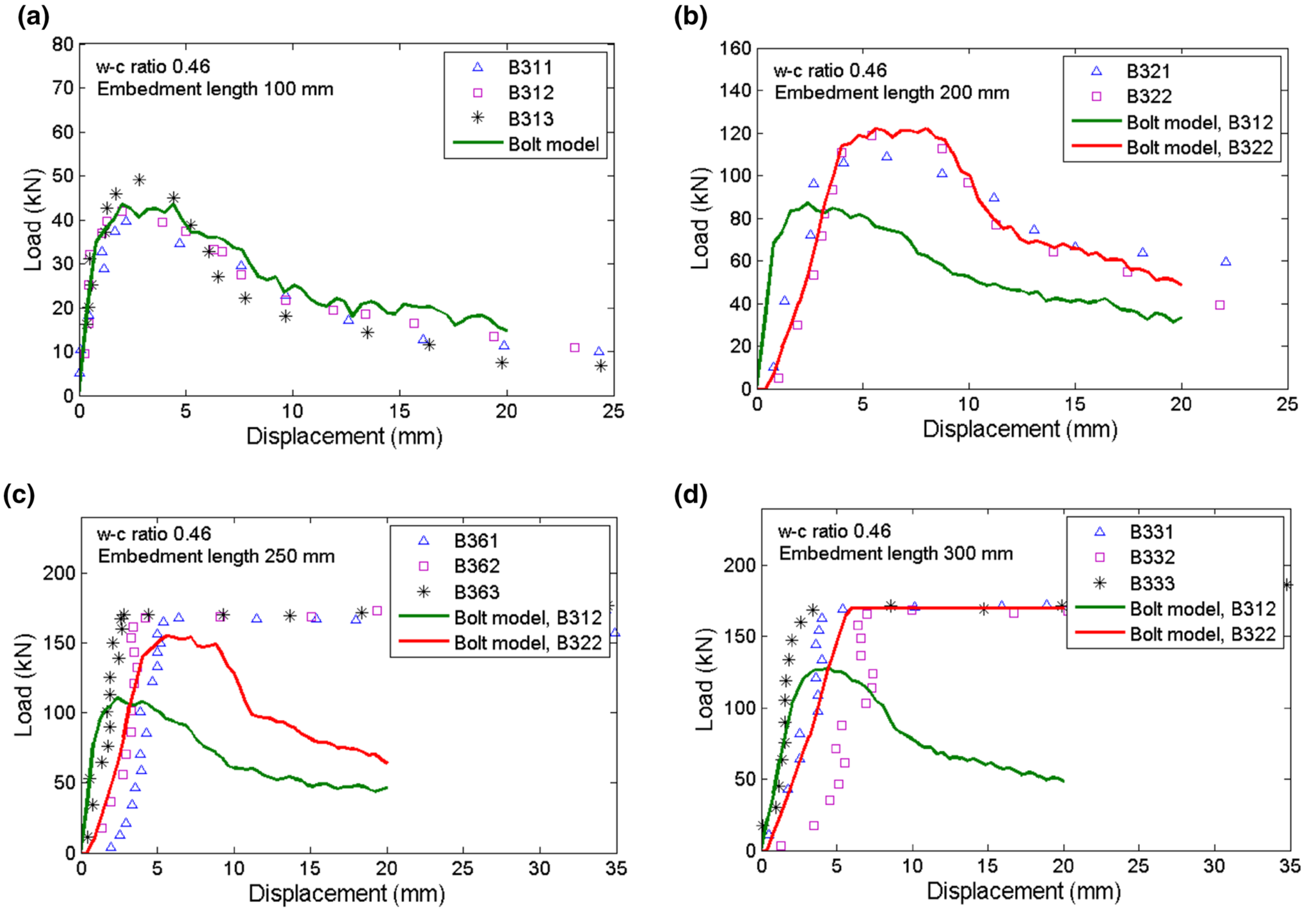

Fig. 13 Load–displacement curves of rockbolts grouted with water–cement ratio of 0.46 in embedment lengths **a** 10 cm, **b** 20 cm, **c** 25 cm, **d** 30 cm

conditions, and the derived bond–slip relationship would therefore reflect the influences of the confining stress.

Conclusions

It is not easy to determine the bond–slip relationship of fully grouted rockbolts, especially when bolts are installed in the field where many factors would influence the shear bonding behavior of rockbolts. One method to estimate the bond–slip relationship of long bolts is to use the short bolts installed under the similar installation and geological conditions. This method is based on two assumptions: (a) The shear bond stress versus shear displacement relationship simply computed from the load–displacement curve of a short grouted bolt is assumed to be able to represent the interfacial bonding characteristics of the short bolt and (b) the bond–slip relationship of a rockbolt is independent of its embedment length and the bond–slip relationship derived from the short bolt is assumed to be able to represent the axial behavior of long grouted bolts.

To evaluate the first assumption, pullout tests were conducted by the authors on strain-gauged rockbolts installed in steel tubes. The bond–slip relationships obtained from the strain measurements and from the load–displacement curves are implemented into numerical rockbolt models. The findings are (1) the measured shear stresses are not uniform along the bolt length for short encapsulated rockbolts; (2) the bond–slip relationship derived from the load–displacement curve is in a reasonable agreement with the average of the measured shear stresses and could predict well the axial behaviors of rockbolts. Hence, the interfacial shear bonding characteristics of a short rockbolt could be simply estimated from its load–displacement curve.

Martin et al. (2011a) and Li et al. (2016)'s bolt pullout tests were used to evaluate the second assumption. The bond–slip relationships obtained from the pullout tests of short grouted bolts are implemented into the numerical rockbolt models. For Martin et al. (2011a)'s test, the numerical bolt model could predict well the axial behavior of a bolt with longer embedment length. For Li et al. (2016)'s tests, the numerical model generates reasonable predictions on

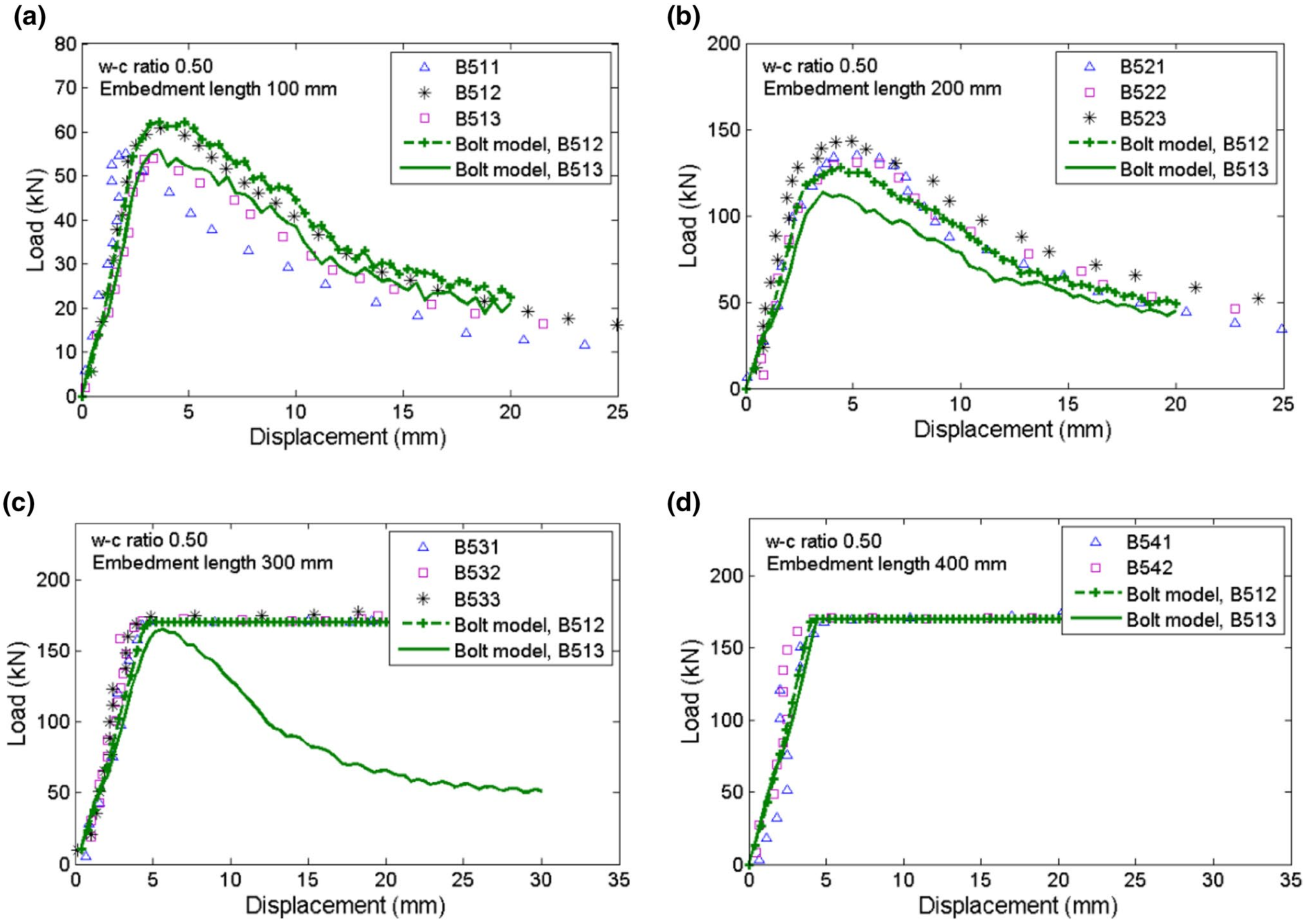

Fig. 14 Load–displacement curves of rockbolts grouted with water–cement ratio of 0.50 in embedment lengths **a** 10 cm, **b** 20 cm, **c** 30 cm, **d** 40 cm

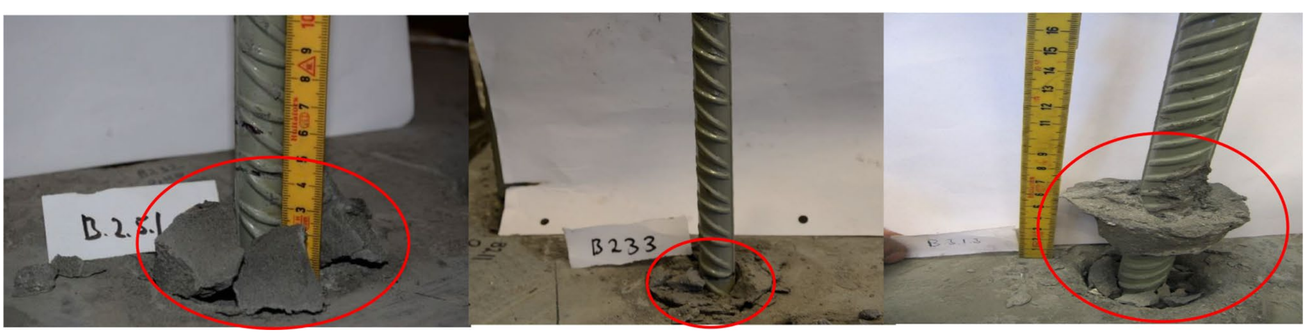

Fig. 15 Concrete fracture occurrence in the bolt pullout test

axial behaviors of long grouted bolts in some cases, but the numerical bolt model underpredicts the axial loads of longer bolts. The bond strength of rockbolts is dependent upon the bolt embedment length for Li et al. (2016)'s tests, which might be caused by the concrete fracture involvement.

In analytical or numerical rockbolt models where the bond–slip relationship is required, a series of pullout tests on short encapsulated rockbolts need to be conducted with the objective to select an appropriate bond–slip relationship which is able to more accurately model the axial behavior of rockbolts. Further laboratory and field tests need to be carried out to verify the impacts of the embedment length on bonding characteristics, and further studies also need to be performed to determine the bond–slip relationship of rockbolts.

Acknowledgements The authors appreciate the help of the technical staff at the University of Wollongong in conducting the tests. This work was supported by the Open Fund of State Key Laboratory of Geohazard Prevention and Geoenvironment Protection under Grant No. SKLGP2017K007.

Compliance with ethical standards

Conflict of interest No potential conflict of interest was reported by the authors.

References

Aziz N (2004) Bolt surface profiles—an important parameter in load transfer capacity appraisal. In: International symposium on ground support, Perth, Western Australia, pp 221–231

Benmokrane B, Chennouf A, Mitri H (1995) Laboratory evaluation of cement-based grouts and grouted rock anchors. Int J Rock Mech Min Sci Geomech Abstr 32:633–642

Chen Y, Li C (2015) Performance of fully encapsulated rebar bolts and D-Bolts under combined pull-and-shear loading. Tunn Undergr Space Technol 45:99–106. https://doi.org/10.1016/j.tust.2014.09.008

Deb D, Das K (2011a) Modelling of fully grouted rock bolt based on enriched finite element method. Int J Rock Mech Min Sci 48:283–293. https://doi.org/10.1016/j.ijrmms.2010.11.015

Deb D, Das K (2011b) Enriched finite element procedures for analyzing decoupled bolts installed in rock mass. Int J Numer Anal Methods Geomech 35:1636–1655. https://doi.org/10.1002/nag.970

Ghadimi M, Shahriar K, Jalalifar H (2015) Optimization of the fully grouted rock bolts for load transfer enhancement. Int J Min Sci Technol 25:707–712. https://doi.org/10.1016/j.ijmst.2015.07.002

Huang M, Zhou Z, Ou J (2014) Nonlinear full-range analysis of load transfer in fixed segment of tensile anchors. Chin J Rock Mech Eng 33(11):2190–2199

Itasca (2006) FLAC—fast Lagrangian analysis of continua. Version 5. Itasca Consulting Group Inc

Ivanović A, Neilson R (2009) Modelling of debonding along the fixed anchor length. Int J Rock Mech Min Sci 46:699–707

Kilic A, Yasar E, Celik A (2002) Effect of grout properties on the pull-out load capacity of fully grouted rock bolt. Tunn Undergr Space Technol 17:355–362

Kristjansson G (2014) Rock bolting and pull out test on rebar bolts. Norwegian University of Science and Technology, Master of Degree

Li C, Stillborg B (1999) Analytical models for rock bolts. Int J Rock Mech Min Sci 36:1013–1029

Li C, Kristjansson G, Høien A (2016) Critical embedment length and bond strength of fully encapsulated rebar rockbolts. Tunn Undergr Space Technol 59:16–23. https://doi.org/10.1016/j.tust.2016.06.007

Li F, Quan X, Jia Y, Wang B, Zhang G, Chen S (2017a) The experimental study of the temperature effect on the interfacial properties of fully grouted rock bolt. Appl Sci 7:327

Li F, Jin H, Hu D, Wang B, Jia Y (2017b) Influence of temperature and roughness of surrounding rocks on mechanical behavior of rock bolts. Soil Dyn Earthq Eng 103:55–63. https://doi.org/10.1016/j.soildyn.2017.09.011

Liu J, Yang H, Wen H, Zhou X (2017) Analytical model for the load transmission law of rock bolt subjected to open and sliding joint displacements. Int J Rock Mech Min Sci 100:1–9. https://doi.org/10.1016/j.ijrmms.2017.01.018

Lu W, Zhao D, X Mao, Ai Y (2018) Experimental study on bond–slip behavior of bamboo bolt-modified slurry interface under pull-out load. Adv Civ Eng 2018:23. https://doi.org/10.1155/2018/6960285

Ma S, Nemcik J, Aziz N (2013) An analytical model of fully grouted rock bolts subjected to tensile load. Constr Build Mater 49:519–526. https://doi.org/10.1016/j.conbuildmat.2013.08.084

Ma S, Nemcik J, Aziz N (2014a) Simulation of fully grouted rockbolts in underground roadways using FLAC2D. Can Geotech J 51:911–920

Ma S, Nemcik J, Aziz N, Zhang Z (2014b) Analytical model for rock bolts reaching free end slip. Constr Build Mater 57:30–37. https://doi.org/10.1016/j.conbuildmat.2014.01.057

Ma S, Nemcik J, Aziz N, Zhang Z (2016) Numerical Modeling of fully grouted rockbolts reaching free-end slip. Int J Geomech 16(1):04015020. https://doi.org/10.1061/(ASCE)GM.1943-5622.000048

Ma S, Zhao Z, Nie W, Gui Y (2016) A numerical model of fully grouted bolts considering the tri-linear shear bond–slip model. Tunn Undergr Space Technol 54:73–80. https://doi.org/10.1016/j.tust.2016.01.033

Martin L, Hassen F, Tijani M, Noiret A (2011a) A new experimental and analytical study of fully grouted rockbolts. In: 45th US rock mechanics/geomechanics symposium, San Francisco, United States, ARMA, pp 11–242

Martin L, Tijani M, Hadj-Hassen F (2011b) A new analytical solution to the mechanical behaviour of fully grouted rockbolts subjected to pull-out tests. Constr Build Mater 25:749–755

Meng Q, Han L, Sun J, Min F, Feng W, Zhou X (2015) Experimental study on the bolt–cable combined supporting technology for the extraction roadways in weakly cemented strata. Int J Min Sci Technol 25:113–119. https://doi.org/10.1016/j.ijmst.2014.11.010

Nemcik J, Ma S, Aziz N, Ren T, Geng X (2014) Numerical modelling of failure propagation in fully grouted rock bolts subjected to tensile load. Int J Rock Mech Min Sci 71:293–300

Ren F, Yang Z, Chen J, Chen W (2010) An analytical analysis of the full-range behaviour of grouted rockbolts based on a tri-linear bond–slip model. Constr Build Mater 24:361–370

Salemi A, Sereshki F, Esmaeili M (2017) Investigating the mechanical performance of contact point in bolted segments by laboratory tests. Eur J Environ Civ Eng 21:148–171. https://doi.org/10.1080/19648189.2015.1110053

Tan C (2016) Difference solution of passive bolts reinforcement around a circular opening in elastoplastic rock mass. Int J Rock Mech Min Sci 81:28–38. https://doi.org/10.1016/j.ijrmms.2015.11.001

Wu Z, Yang S, Zheng J, Hu X (2010) Analytical solution for the pullout response of FRP rods embedded in steel tubes filled with cement grout. Mater Struct 43(5):597–609

Yang S, Huang W, Liu Y (2014) Push-out test to study bond properties of mortar–concrete interface. Mag Concr Res 66:1104–1115. https://doi.org/10.1680/macr.14.00076

Zheng Y, Guo Z, Liu J, Chen X, Xiao Q (2016) Performance and confining mechanism of grouted deformed pipe splice under tensile load. Adv Struct Eng 19:86–103. https://doi.org/10.1177/1369433215618296